Excitation and Evolution of the Quasi-2-Day Wave Observed in *UARS*/MLS Temperature Measurements

D. L. WU, E. F. FISHBEIN, W. G. READ, AND J. W. WATERS

Jet Propulsion Laboratory, California Institute of Technology, Pasadena, California

(Manuscript received 9 June 1995, in final form 12 September 1995)

ABSTRACT

The quasi-2-day wave is known as a strong and transient perturbation in the middle and upper atmosphere that often occurs shortly after solstice. The excitation mechanisms of this transient wave have been discussed for years, but no clear answer has yet been attained. In this paper, propagating characteristics of the 2-day wave are studied based on 8-mon temperature measurements from the Microwave Limb Sounder onboard the *Upper Atmosphere Research Satellite*. The studies are focused on the wave events that happened in January 1993 and in July–August 1993. The observations suggest that winter planetary waves could be responsible for triggering the summer 2-day wave through long penetration into the summer stratosphere. A connection is evident in the evolution of the wave amplitude between the summer 2-day wave generation and winter wave penetration. The data also suggest that the enhancement of the wave amplitude is a manifestation of both a local unstable wave and a global normal-mode Rossby wave.

1. Introduction

The quasi-2-day wave is a global westward traveling oscillation often observed in the middle and upper atmosphere during the months of January–February and July–August. The 2-day oscillation has been found in mesospheric wind measurements above 80–100 km at a number of ground-based radar stations (e.g., Müller and Kingsley 1974; Craig and Elford 1981; Tsuda et al. 1988) as well as in upper-stratospheric rocketsonde winds (Coy 1979). Satellite temperature and wind measurements (Rodgers and Prata 1981; Burks and Leovy 1986; Wu et al. 1993) are able to provide a global view of the phenomenon and associate it with zonal wavenumber 3–4 structures. The 2-day wave appears to be a relatively strong perturbation at midlatitudes during solstice periods and has several interesting features. It occurs intermittently with a lifetime of 10–30 days, and the wave events usually peak 1 mo after solstice in the summer hemisphere. The wave period varies from 1.8 to 2.3 days with larger frequency variability in July–August events.

Two mechanisms have been proposed to explain the wave excitation. One is known as the normal-mode theory (Salby 1981) that interprets the 2-day oscillation as a manifestation of the (3, 0) Rossby normal mode. In the real atmosphere, the structure of a resonant normal mode may be distorted in shape due to nonuniform mean winds. A small perturbation such as atmospheric instability and breaking planetary waves may excite a global normal-mode response if the atmospheric conditions are favorable. Atmospheric viscosity is the damping mechanism that prevents normal modes from indefinite growth. Another explanation for the 2-day wave emphasizes the role of the baroclinic instability above the summer easterly jet (Plumb 1983). According to this theory, the 2-day wave is one of fast-growing unstable modes, and its enhancement is localized in baroclinically unstable zones. A perturbation may grow widely in a short period of time if it matches an unstable mode in wavenumber and frequency.

It is also possible that the 2-day wave exists as a combination of normal and unstable modes. As suggested by Randel (1994), the observed wave structures, on one hand, agree well with normal-mode calculations showing an expected (3, 0) structure in the summer hemisphere and a consistent phase relation across the two hemispheres. On the other hand, the episode of the summer 2-day wave is well correlated with the local instability signature in the 5-yr observations. The matches of the (3, 0) normal mode and unstable waves in frequency and wavenumber make the 2-day wave components difficult to distinguish from one another. In fact, the coupling of normal-mode and baroclinic instabilities enables the 2-day wave to be more readily excited in solstice periods. The forcings leaking from the winter into the summer hemisphere have been suggested as being responsible for the initial triggering (Tsuda et al. 1988; Craig et al. 1980).

In this paper, we present new evidence of excitation and evolution of the 2-day wave observed in the temper-

Corresponding author address: Dr. Dong L. Wu, Jet Propulsion Laboratory, California Institute of Technology, 4800 Oak Grove Dr., Pasadena, CA 91109.

ature measurements with the Microwave Limb Sounder (MLS) onboard the *Upper Atmosphere Research Satellite* (*UARS*). Evolution of the 2-day wave in a high temporal resolution is obtained to study the cause and effect relation of the propagating disturbance. Behaviors of the wave propagation are found to be consistent with the suggestion that the 2-day wave is composed of both normal and unstable modes during its development. A connection between the summer 2-day wave and the winter wave is evident in the MLS data, a possible signature of the winter wave leaking into the summer hemisphere and triggering the summer 2-day wave.

2. Data

The data analyzed here are obtained with special research algorithms developed by the MLS science team to improve temperature and pressure retrievals. The MLS, in operation since 12 September 1991, is a remote sensing instrument designed to simultaneously measure molecular abundances (O_3, ClO, H_2O, and HNO_3), temperature, and pressure in the middle atmosphere (Waters 1993; Barath et al. 1993). Temperature and pressure are retrieved from the radiance measurements of O_2 microwave thermal emissions near 63 GHz, of which the line spectrum is resolved into 15 channels. In the standard MLS products, version 3 (V3) currently available to the public, temperature is retrieved at six pressure levels from 22 to 0.46 mb. With some modifications, temperature is retrieved at 10 pressure levels in this new algorithms adding 46, 0.22, 0.1, and 0.046 mb.

The basic principle of temperature retrieval is the same in both the new and standard algorithms (Fishbein et al. 1995). The major differences, which lead to better results for temperature, are in the treatments of background emissions and radiance measurements near the line center. The new temperature results, although still preliminary, are improved in several aspects: 1) The systematic bias due to background emissions is greatly reduced. There was an ~1 K systematic variation synchronized to the *UARS* yaw cycle in the V3 temperature. A better model is applied in the new algorithms to remove the nonatmospheric contributions, reducing the bias to less than 0.3 K. 2) Temperatures at 0.22, 0.1, and 0.046 mb are being retrieved for scientific uses. The temperature information at these levels comes primarily from the radiance close to the line center, which is measured with three channels. The three center channels are excluded in the V3 software to avoid possible contamination of Zeeman splitting due to the earth's magnetic field. However, in the new algorithms we take advantage of the fact that the saturated radiance is a weak function of the Zeeman effect and include the three-channel radiance measurements in the temperature retrieval. As a result, we obtain some useful temperature measurements at higher altitudes. 3) In the new algorithms, temperature retrieval is coupled with pressure retrieval in a vector format. The vector scheme improves both pressure and temperature retrievals at high altitudes because it prevents retrieval errors from propagating to low altitudes as inherent in the onion-peeling type of retrievals employed by the V3 software. 4) The new temperature product is now independent of the NMC (National Meteorological Center, now National Centers for Environmental Prediction) analyses. Instead of relaxing to the NMC data, the new product is constrained to a *UARS* climatology when there is no temperature information from the radiance measurements. Therefore, the new product is more valuable for applications in data assimilation.

The bias due to the earth's magnetic field is estimated in the new retrieval, and special consideration has been given to potential errors because the algorithms do not account for the Zeeman splitting effect. In principle, temperature may be retrieved up to ~0.005 mb if the Zeeman effect is accurately calculated. However, at the present time, modeling the Zeeman effect is limited to a few simple calculations that are not adequate to deal with complicated magnetic field orientations. Given the existing forward model calculations, temperatures up to the 0.022-mb level may still be retrieved using MLS saturated radiances. Such retrievals, without sophisticated computations of the magnetic effect, may produce some scientifically useful results, but additional errors need to be quantitatively assessed. The errors are estimated and listed in Table 1 for selected pressure levels. Since the effect of the magnetic field is approximately constant for the MLS sampling at a given latitude cycle, the error introduces less contamination to the study of fast-moving waves than the study of slowly moving waves. In other words, waves 2 and 3 are less affected than wave 1 and mean components. The confidence level for the 2-day wave amplitudes obtained in this study is about 0.5 K at heights below 0.46 mb and 1 K above that height.

TABLE 1. Estimated errors in data retrieved from MLS observations.

Pressure level (mb)	Accuracy		Precision in temperature (K)			
	Pressure (m)	Temp (K)	Diurnal and yaw cycle	Magnetic field effects		
				Mean	Wave 1	Wave 2
0.046	70	5	<0.3	8	8	<2
0.1	40	6	<0.3	5	5	<1
0.22	30	4	<0.3	2	2	<0.5
0.46	20	1.5	<0.3	<0.5	<0.5	0
1	20	1	<0.3	0	0	0
2.2	30	0.8	<0.3	0	0	0
4.6	40	0.6	<0.3	0	0	0
10	60	0.7	<0.3	0	0	0
22	120	1	<0.3	0	0	0
46	180	2	<0.3	0	0	0

The MLS-sampled latitudes range from 34° in one hemisphere to 80° in the other, and two solar local times are sampled at a given latitude circle. The spacecraft makes 10 yaw maneuvers per year, allowing views of the polar regions alternately. There are 15 orbits per day and about 90 profiles per orbit. The data during 30 November 1992–17 September 1993 are analyzed, and two solstice periods are covered with continuous observations.

3. Wave spectra

The MLS temperature data, gridded in latitude and pressure level, are subject to spectral analysis to extract zonally propagating wave perturbations. A wave spectrum, which is defined here as the amplitude response at a given frequency and wavenumber, is calculated using a least squares fitting technique (Wu et al. 1995). Aliasing is also examined for the different sampling patterns at various latitudes. For *UARS*, there are enough samples to resolve a wave-3 structure such that the 2-day wave is generally not aliased by other major planetary waves. However, in the high-latitude stratosphere winter, planetary waves are so strong and rich in spectrum that the spectral power leakage may not be neglected. In most cases, the 2-day wave is a well-defined spectral component and easily resolved.

Figure 1 presents the wave spectrum at a latitude of 20°S and a pressure level of 0.46 mb for the period of 10–30 January 1993, when the 2-day wave sharply peaks at a period of ~48 h and zonal wavenumber 3 as a westward traveling oscillation. The 48-h period derived from the MLS temperature data is consistent with previous observation (Rodgers and Prata 1981; Randel 1994). The 2-day wave period, as suggested by normal-mode calculations (Salby 1981; Hagan et al. 1993), may vary slightly if the structure of mean flow changes, and multiple spectral components may also be present. Nevertheless, these calculations suggest that the prominent spectral component of the January event should be close to the 48 h that agrees with most observations. The 2-day wave may not be easily identified from temperature anomaly maps because, as seen in Fig. 1, other planetary waves are also present, such as the diurnal tide, a westward propagating 10-day wave, and the stationary wavenumber 1.

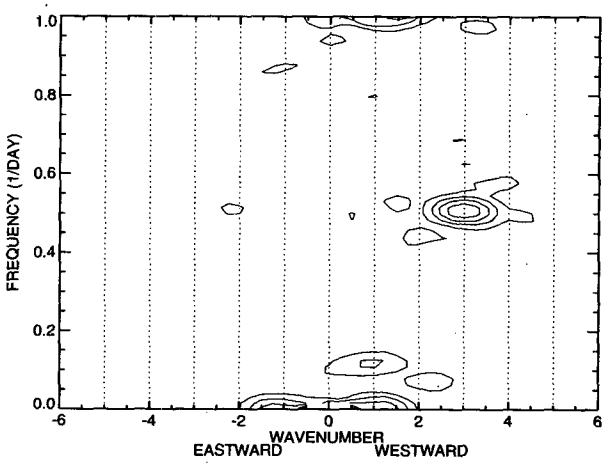

FIG. 1. Wave spectrum for the period 10–30 January 1993 at latitude 20°S and pressure 0.46 mb, where the 2-day wave sharply peaked at a period of ~48 h and wavenumber 3. Contours describe the amplitude responses at each frequency and wavenumber and start from a value of 0.5 K with an increment of 0.5 K. The confidence level is ~0.5 K for the amplitude response near the 2-day wave.

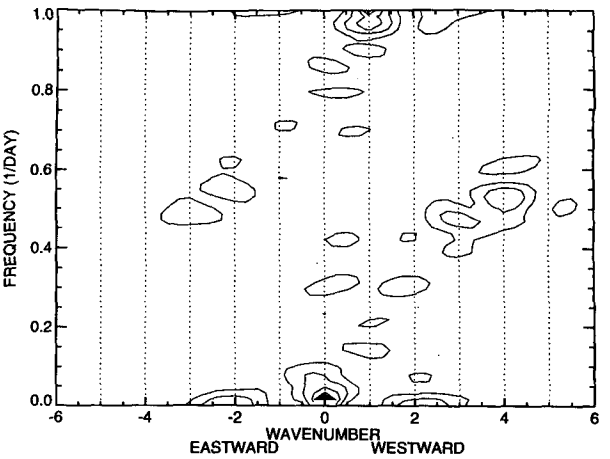

FIG. 2. Wave spectrum for the period 18 June–7 July 1993 at latitude 20°N and pressure 0.1 mb. Contours start from 0.4 K with an increment of 0.4 K. Two wave components are identified for the 2-day wave event and they are the periods of 50 h for wave 3 and 45 h for wave 4, respectively.

Figure 2 is the wave spectrum at a latitude of 20°N and a pressure level of 0.1 mb for the period of 18 June–7 July 1993. This is a much weaker event than that in January and consists of two equally important spectral components. One component peaks at a period of ~50 h and zonal wavenumber 3, while another can be identified at a period of ~45 h and zonal wavenumber 4, compared to 41 h found by Rodgers and Prata (1981) for the month of July. These values are somewhat different from 58 and 55 h found in the NCEP temperature data (Randel 1994), but there is consistency showing that the shorter period is also associated with the larger wavenumber. Some aliases are also present in the spectrum because this sampling pattern is different from the case in January 1993. The weaker amplitudes, located at (wavenumber, period) = (−3, ~0.49) and (−2, 0.53), are, respectively, the aliases of the 2-day wave components at (4, 0.53) and (3, 0.48). Aliasing arises because two nodes sampled at this latitude circle are too close together in local time. Since the aliasing is not mutually equal in amplitude, we are able to distinguish the aliasing and aliased com-

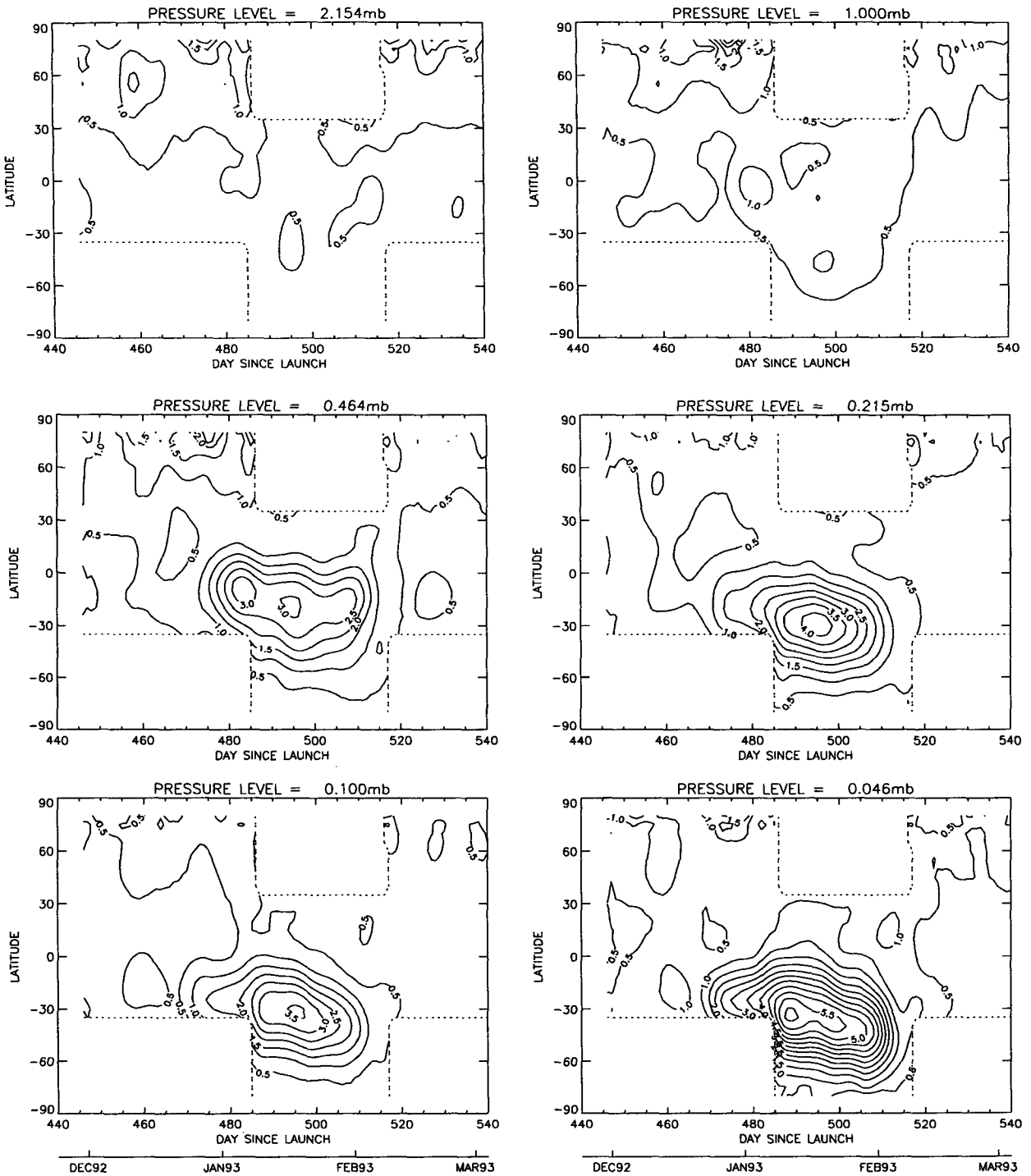

FIG. 3. Evolution of the January 2-day wave for the component at (wavenumber, frequency) = (3, 0.5). Contours are labeled from 0.5 K with an increment of 0.5 K. The confidence level is estimated to be 0.5 K for most pressure levels from 46 to 0.046 mb. The dashed lines show the boundary of MLS sampling, which is biased to the different hemispheres alternately as a result of the *UARS* yaw maneuvers.

ponents. Multiple wave components were also observed in mesospheric radar winds during the month of July 1991 (Harris and Vincent 1992), where periods of 51 and 44 h were specified.

4. The 2-day wave in January 1993

The 2-day wave amplitudes and phases are extracted at the two prominent frequencies, that is (3, 0.5) and

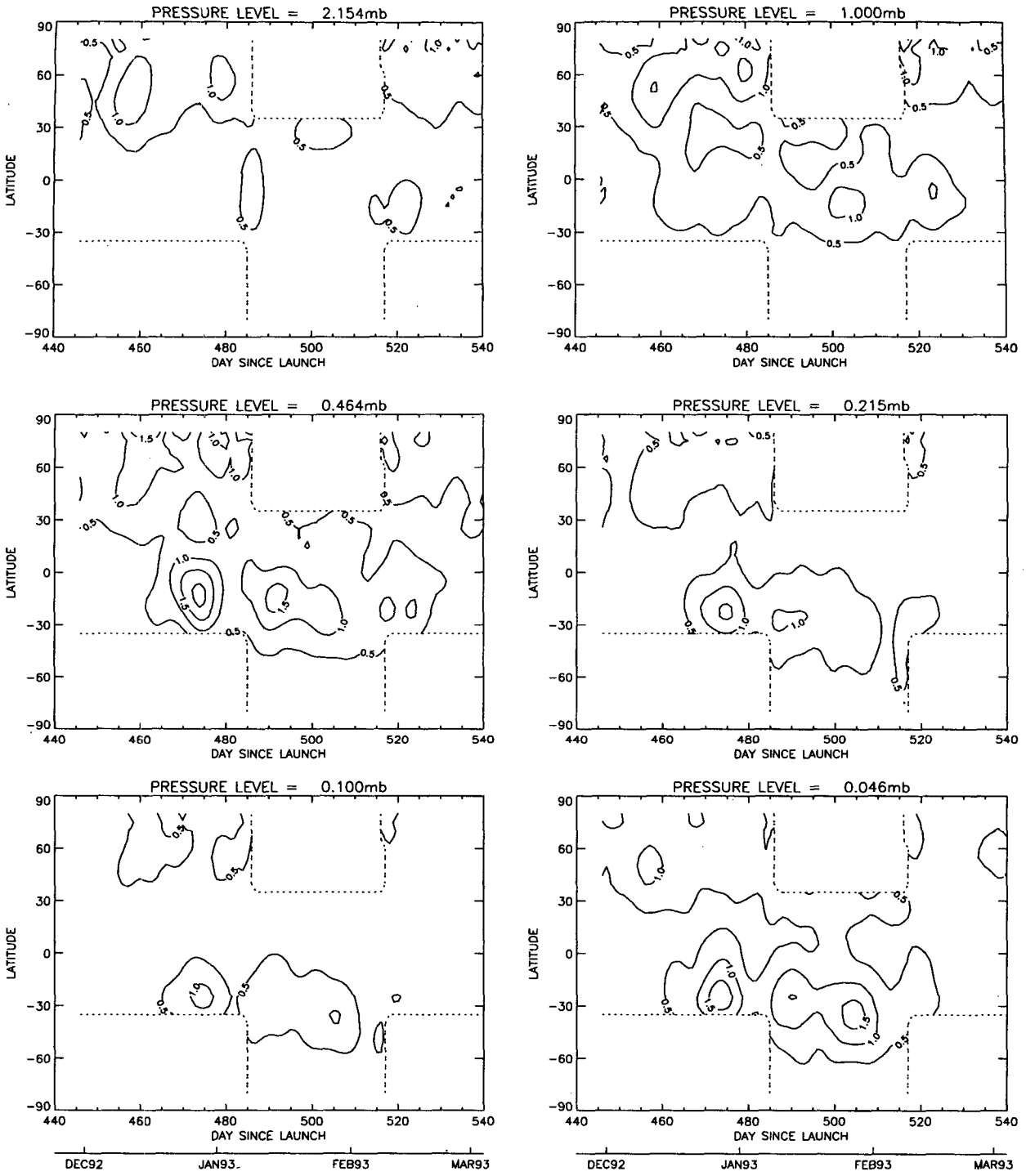

FIG. 4. As in Fig. 3 but for the component (4, 0.53).

(4, 0.53), using the aforementioned least squares method. For the January event, time series of the wave amplitudes at (3, 0.5) and (4, 0.53) are shown in Figs. 3 and 4, respectively. In order to investigate detailed generation and evolution processes, the 4-day resolution is specified so that the wave progression can be resolved precisely. Knowing the direction of wave progression, we are able to investigate, to a better extent, cause and effect relations among the 2-day wave, instability, and other planetary waves.

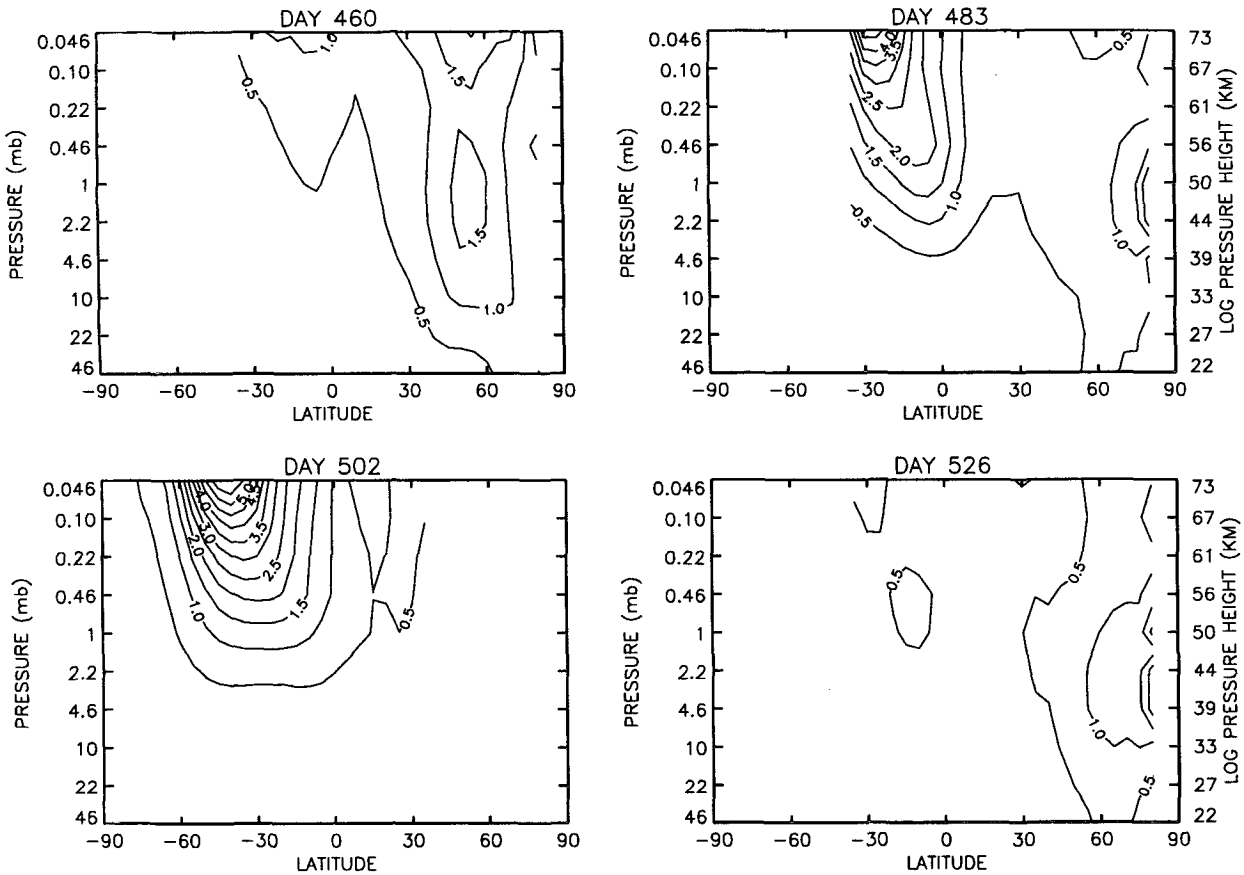

FIG. 5. Latitude–altitude cross section of the 2-day wave amplitude for selected days during the January event. Contours start from 0.5 K at an interval of 0.5 K. A shift in peak amplitude is evident for most of the days, which shows the peak amplitude moving to a higher latitude as the 2-day wave grows into a higher altitude. A burst in the Northern Hemisphere on day 460 is a strong forcing that may be able to penetrate into the summer hemisphere to trigger the 2-day wave.

The time series in Fig. 3 includes the very early stage of the 2-day wave generation for the event in late 1992 and early 1993. A precursor in the Northern Hemisphere around 10 December 1992 can be seen at these pressure levels, which gathers strength throughout the winter and finally spreads to the equator. A second strong disturbance in the Northern Hemisphere occurred near the end of December, which shows a similar radiating pattern in the two hemispheres. These transient winter perturbations seem to connect with some weak and delayed perturbations in the summer hemisphere, as indicated by the southward progression of the wave amplitudes. The delay effect is clearly shown at the levels of 2.2 and 1 mb, where the peak amplitudes at middle latitudes show up later than those at high latitudes. The (3, 0.5) component grew particularly fast at midlatitudes (10°–50°S), and the amplitude peak drifted gradually poleward from 20°S in early January to 30°S in late January. The amplitude peak also drifted to a higher latitude as height increased. After an ~7 K maximum was reached in mid- and late January at 0.046 mb, the 2-day oscillation vanished within a few days in the beginning of February, yielding a total duration time of about 40 days.

The horizontal structure of the January 2-day wave matches the characteristics of the (3, 0) normal mode with a node near the equator. In fact, it will be shown later that the perturbations in the two hemispheres are coherent in phase. At the altitudes below 2 mb, the amplitudes are larger in the winter than in the summer, likely because of the amount of energy dispersed from the wintertime planetary waves. This energy may be responsible for the excitation of the 2-day wave. At the altitudes above 2 mb, the amplitude of the summer wave is larger than that in the winter, which is expected theoretically as the (3, 0) normal mode. It is interesting to note that the enhancement in the summer hemisphere does not immediately follow the first precursor and that the actual burst occurred about 10 days later.

The (4, 0.53) component is weaker in amplitude but accountable as a part of the event throughout the month of January (Fig. 4). Unlike the (3, 0.5) component, the

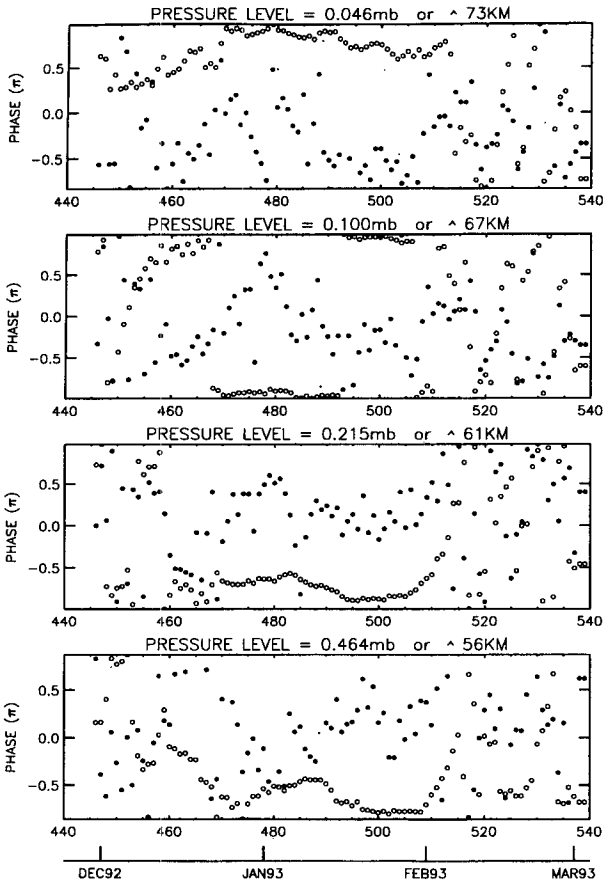

FIG. 6. Time series of the 2-day wave phases at 20°S (circles) and 20°N (filled circles) for selected pressure levels 0.46, 0.22, 0.1, and 0.046 mb. The out-of-phase relation at these levels suggests the existence of the global (3, 0) Rossby normal mode.

amplitude of the (4, 0.53) component is maximized three times in late December, early January, and early February, but the amplitude decreased gradually after the first maximum. It is interesting to observe that the first peak was reached earlier than the time when the (3, 0.5) component began to grow, which may suggest some interactions between the two components. A precursor is also evident in the winter hemisphere at about the same time and place as in the (3, 0.5) component and may be responsible for some later perturbations in the summer hemisphere. The time delay between the perturbations in the two hemispheres again suggests the possible penetration of winter planetary waves into the summer.

Figure 5 displays the latitude–altitude view of the wave amplitude for the January event, where the connection between the summer and winter components is apparent. Day 460 is the time when a strong precursor was observed in the winter hemisphere. The structure of the wave amplitude (Fig. 5a) shows that the winter forcing is radiating away from the polar region to the equatorial area and possibly farther into the summer hemisphere. During the enhancement period, for example day 502, the wave exhibits large strength in the summer hemisphere, with a flat/sharp distribution at lower/higher altitudes. At 0.1 mb (~67 km), the wave amplitude does not exceed 5 K, which is much smaller than the 20 K suggested by the model (Hagan et al. 1993) that is in good agreement with *UARS* High Resolution Doppler Imager (HRDI) wind results (Wu et al. 1993). However, it is noteworthy that the MLS results do not reveal the peak altitude of the wave amplitude, and a large amplitude gradient actually is observed between 50 and 75 km. Therefore, a slight shift in altitude can cause large differences in amplitude comparisons. As is also suggested by the HRDI results, it would give better comparisons if one lowers the model altitude registration slightly.

Figure 6 shows time series of the wave phases at 20°N and 20°S for different pressure levels, revealing coherence of the perturbations in the different hemispheres. A clear out-of-phase relation is evident during the event and agrees reasonably well with the phase structure of the (3, 0) Rossby normal mode. In the real atmosphere, the (3, 0) amplitude may have a node slightly away from the equator, but the summer component is more enhanced than the other (Salby 1981). Phases are expected to be tilted with respect to height, which is observed in Fig. 6, suggesting that the perturbation is propagating upward. Hence, energy and momentum may be transported by the 2-day wave from the winter at low heights into the summer at high altitudes. Coupled to the baroclinic instability above the easterly core, the summer perturbation may grow very rapidly in the unstable region since the unstable waves and the normal mode match in frequency and wavenumber. It is the similarity of the two modes that allows the 2-day wave to develop more efficiently into a global oscillation in the real atmosphere.

The time series of amplitude profiles helps to illustrate the effects of the baroclinic instability in the summer hemisphere. Figure 7 shows a time series of the (3, 0.5) amplitude profiles at 25°S. Two transient forcings, occurring approximately on days 455 and 467, are related to the first precursor discussed above. The peak amplitudes of the two major forcings are tilted with respect to time, suggesting that these disturbances were propagating upward. These forcings may be crucial to the 2-day wave excitation because enhancement is observed following the forcings. After the 2-day wave was triggered, the wave amplitude is first enhanced at a higher altitude, and the enhancement progresses downward, indicated by the downward-tilted contour lines. In other words, the disturbance is effectively enhanced first in dynamically unstable regions when there is enough energy. The location of the unstable regions is consistent with the description provided by the baroclinic instability theory on the summer easterly jet (Plumb 1983; Pfister 1985).

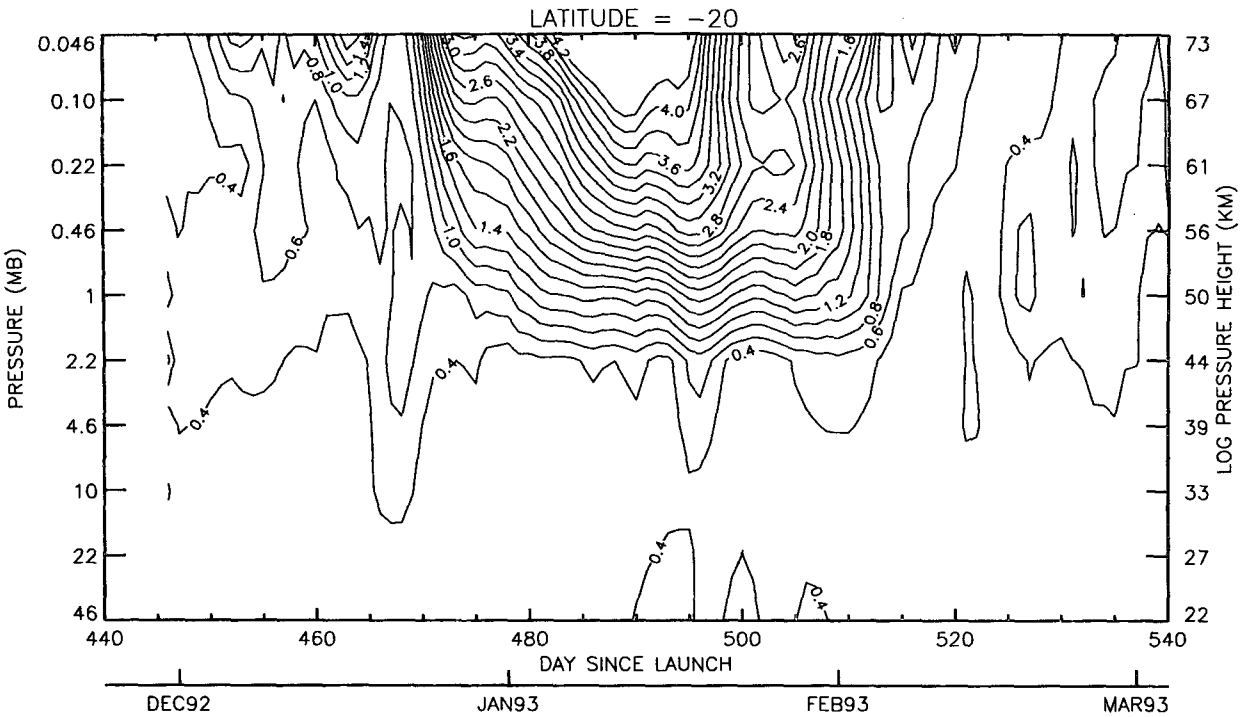

FIG. 7. Time series of the 2-day wave amplitude profiles at a latitude of 20°S, showing the upward propagating disturbances in the early time of the event and the downward progression during the major wave enhancement. The upward and downward propagation may suggest that the 2-day wave is a combination of the normal and unstable modes.

5. The 2-day wave in July–August 1993

The morphology of the 2-day wave during this period is not quite a mirror image of what happened in January 1993 for the MLS temperature measurements. As shown in Figs. 8 and 9, the events in June–August are generally smaller in amplitude and more sporadic in time. It is known that there is large frequency variability during this period of time, and in the MLS data two prominent components at (3, 0.48) and (4, 0.53) for zonal waves 4 and 3 are equally important during this period. For the (3, 0.48) component, illustrated in Fig. 8, major events occurred on days 655, 675, 681, 691, and 705. For the (4, 0.53) component in Fig. 9, major events occurred less frequently and peaked on days 662, 680, and 705.

During July and August 1993, the winter wave is weaker than that in January, indicated by smaller amplitudes that hardly spread across the equator. However, there is no clear evidence of any precursors or connections between the winter and the summer waves during this period although some variability is exposed in the winter hemisphere. The evolution of the (3, 0.48) component, for example at 0.046 mb, is similar to that in the January event in terms of the poleward movement of the peak amplitude. The evolution of the (4, 0.53) component, however, shows that the movement is poleward during June and July. In August, the peak amplitudes tend to be stabilized at ~30°N.

It is not yet clear at the present time why the 2-day wave in July–August is weaker than that in January. The phenomenon may be associated with the strength of baroclinic instability or with the amount of energy from the planetary waves leaking into the summer hemisphere. Solutions given by normal-mode and instability theories are limited. Normal-mode calculations suggest that magnitude of the wave response is proportional to the magnitude of the input perturbation but also sensitive to the mean wind structure, while calculations of unstable waves provide only a growth rate in linearly developing stage but say nothing of their final state. The MLS observations suggest that the amplitude of the summer 2-day wave is proportional to the amount of energy radiated and dispersed from the winter planetary waves. If this is the case, it is not surprising to observe a weaker 2-day wave in July–August because the winter wave activity is known to be stronger in the Northern than in the Southern Hemisphere.

6. Summary and discussion

Using the latest research algorithms, we are now able to retrieve MLS temperatures in a broader height range (46–0.046 mb) and obtain useful information for the 2-day wave study. Observations of the 2-day wave in MLS temperature measurements provide new evidence for excitation and evolution of the transient oscillation. Spectral analysis reveals that there is one major com-

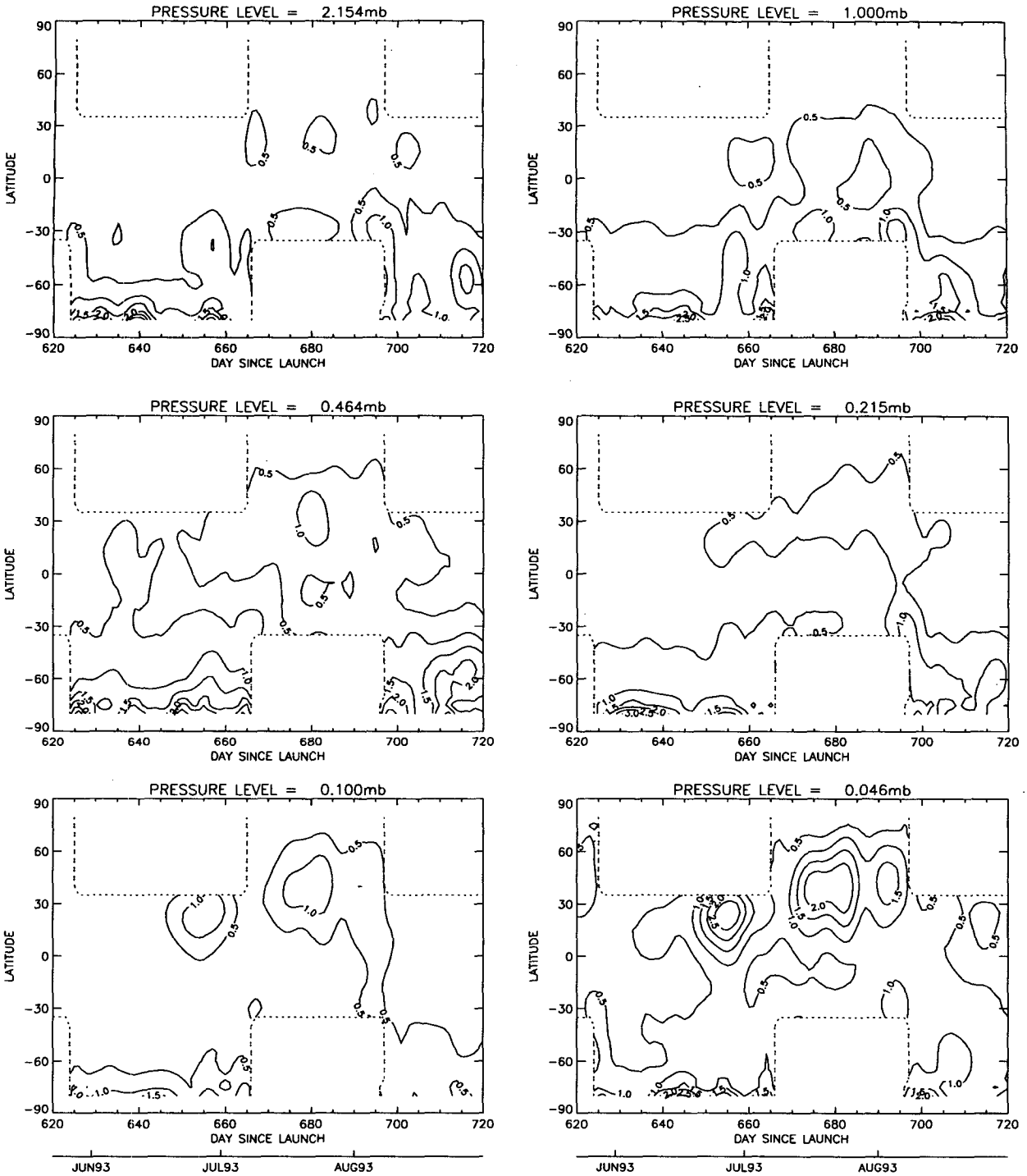

FIG. 8. Evolution of the July–August 2-day wave for the component at (3, 0.48). Sporadic events are found throughout an approximately 2-mo period between mid-June and mid-August. The amplitudes of these events are generally much weaker than the primary event in January 1993.

ponent for the January event and two prominent wave components for the July–August events, results that are consistent with past observations. The 2-day wave in January 1993 appears to be dominated by wave 3, while waves 3 and 4 are both important for the events in July–August 1993.

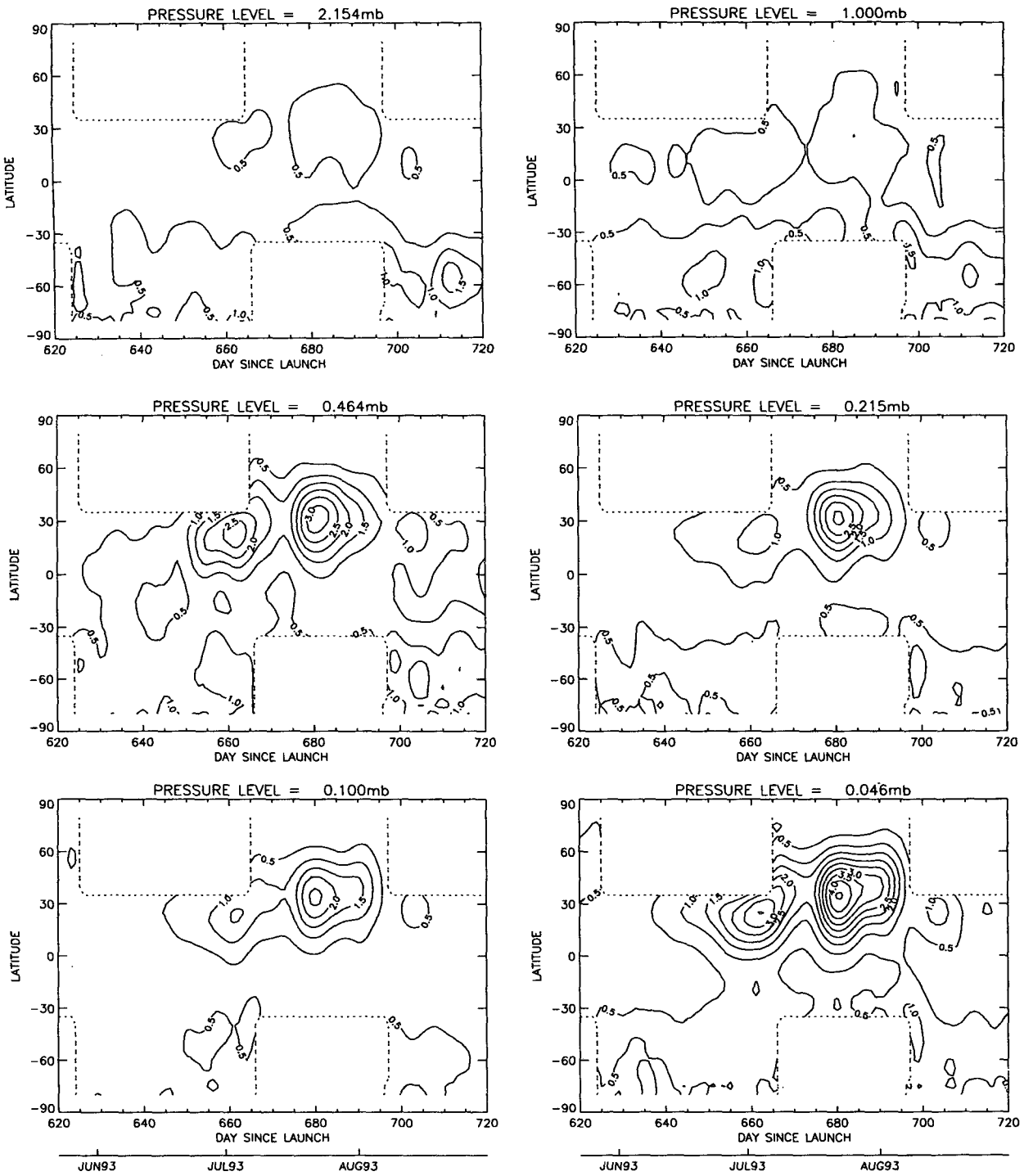

FIG. 9. As in Fig. 8 but for the component at (4, 0.53). The amplitude response of this component is about twice as large as that of the (3, 0.48) component for most events that happened in this time.

The wave amplitude and phase structures extracted from the MLS temperatures suggest a possible connection between the summer 2-day wave and the winter planetary wave activity. A precursor in the winter hemisphere is found likely to be a triggering signature for the summer 2-day wave enhanced in January. The study of the wave evolution suggests that the 2-day wave is possibly affected by both the winter wave forc-

ings and the summer baroclinic instability above the easterly jet. The wave leaking from the winter into the summer hemisphere may be an important triggering forcing, and such forcing can be easily enhanced by the summer baroclinic instability due to the matched frequencies and wavenumbers between the normal and unstable modes. As a combination of the (3, 0) normal mode and an unstable wave, the 2-day wave may grow and spread efficiently to a wide region in the atmosphere. Randel (1994) also discussed such a possibility of the 2-day wave being a combination of the normal and unstable modes based on a study of 5-yr NMC data. The characteristics of the 2-day wave were found to be mixed with the signatures of the two types of waves and can only be interpreted as the presence of both the normal and unstable modes. The MLS observations show a similar scenario in which the evolution of the 2-day wave contains characteristics mixed with the two types of waves. More important, the MLS observations tend to relate the triggering mechanism of the 2-day wave to the forcings in the winter hemisphere, which may help us to better understand some seasonal variations of the wave.

Acknowledgments. We thank the MLS science team for supporting this study, especially Robert Jarnot, Richard Lay, and Dennis Flower for informative discussions on the instrument calibration and operation. This work was performed at the Jet Propulsion Laboratory, California Institute of Technology, under contract with the National Aeronautics and Space Administration (NASA), and sponsored by NASA through the Upper Atmosphere Research Satellite Project.

REFERENCES

Barath, F. T., and Coauthors, 1993: The Upper Atmosphere Research Satellite Microwave Limb Sounder instrument. *J. Geophys. Res.*, **98,** 10 751–10 762.

Burks, D., and C. Leovy, 1986: Planetary waves near the mesospheric easterly jet. *Geophys. Res. Lett.*, **13,** 193–196.

Coy, L., 1979: A possible 2-day oscillation near the tropical stratopause. *J. Atmos. Sci.*, **36,** 1615–1618.

Craig, R. L., and W. G. Elford, 1981: Observations of the quasi 2-day wave near 90 km altitude at Adelaide (35°S). *J. Atmos. Terr. Phys.*, **43,** 1051–1056.

——, R. A. Vincent, G. J. Fraser, and M. J. Smith, 1980: The quasi 2-day wave in the Southern Hemisphere mesosphere. *Nature,* **287,** 319–320.

Fishbein, E. F., and Coauthors, 1995: Validation of UARS MLS temperature and pressure measurements, *J. Geophys. Res.*, in press.

Hagan, M. E., J. M. Forbes, and F. Vial, 1993: A numerical investigation of the propagation of the quasi 2-day wave into the lower thermosphere. *J. Geophys. Res.*, **98,** 23 193–23 205.

Harris, T. J., and R. A. Vincent, 1993: The quasi-two-day wave observed in the equatorial middle atmosphere. *J. Geophys. Res.*, **98,** 10 481–10 492.

Muller, H. G., and S. P. Kingsley, 1974: On the scale sizes of wind systems in the meteor zone. *J. Atmos. Terr. Phys.*, **36,** 1851–1861.

Pfister, L., 1985: Baroclinic instability of easterly jets with application to the summer mesosphere. *J. Atmos. Sci.*, **42,** 313–330.

Plumb, R. A., 1983: Baroclinic instability of the mesosphere: A mechanism for the 2-day wave? *J. Atmos. Sci.*, **40,** 262–270.

Randel, W. J., 1994: Observations of the 2-day wave in NMC stratospheric analyses. *J. Atmos. Sci.*, **51,** 306–313.

Rodgers, C. D., and A. J. Prata, 1981: Evidence for a traveling two-day wave in the middle atmosphere. *J. Geophys. Res.*, **86,** 9661–9664.

Salby, M. L., 1981: The 2-day wave in the middle atmosphere: Observations and theory. *J. Geophys. Res.*, **86,** 9661–9664.

Tsuda, T., S. Kato, and R. A. Vincent, 1988: Long period wind oscillations observed by the Kyoto meteor radar and comparison of the quasi-2-day wave Adelaide HF radar observations. *J. Atmos. Terr. Phys.*, **50,** 225–230.

Waters, J. W., 1993: Microwave limb sounding. *Atmospheric Remote Sensing by Microwave Radiometry,* M. A. Janssen, Ed., John Wiley & Sons, 383–496.

Wu, D. L., P. B. Hays, W. R. Skinner, A. R. Marshall, M. D. Burrage, R. S. Lieberman, and D. A. Ortland, 1993: Observations of the quasi 2-day wave from the High Resolution Doppler Imager on UARS. *Geophys. Res. Lett.*, **20,** 2853–2856.

——, ——, and ——, 1995: A least squares method for spectral analysis of space–time series. *J. Atmos. Sci.*, **52,** 3501–3511.